A posteriori correction of DG schemes through subcell finite volume formulation and flux recontruction

François Vilar

Institut Montpelliérain Alexander Grothendieck
Université de Montpellier

March 19, 2019

History

- Introduced by Reed and Hill in 1973 in the frame of the neutron transport
- Major development and improvements by B. Cockburn and C.-W. Shu in a series of seminal papers

Procedure

- Local variational formulation
- Piecewise polynomial approximation of the solution in the cells
- Choice of the numerical fluxes
- Time integration

Advantages

- Natural extension of Finite Volume method
- Excellent analytical properties (L_2 stability, $hp-$adaptivity, ...)
- Extremely high accuracy (superconvergent for scalar conservation laws)
- Compact stencil (involve only face neighboring cells)

1D scalar conservation law

- $\dfrac{\partial u}{\partial t} + \dfrac{\partial F(u)}{\partial x} = 0, \qquad (x,t) \in \omega \times [0,T]$
- $u(x,0) = u_0(x), \qquad x \in \omega$

$(k+1)^{\text{th}}$ order discretization

- $\{\omega_i\}_i$ a partition of ω, such that $\omega_i = [x_{i-\frac{1}{2}}, x_{i+\frac{1}{2}}]$
- $0 = t^0 < t^1 < \cdots < t^N = T$ a partition of the temporal domain $[0,T]$
- $u_h(x,t)$ the numerical solution, such that $u_{h|\omega_i} = u_h^i \in \mathbb{P}^k(\omega_i)$

$$u_h^i(x,t) = \sum_{m=1}^{k+1} u_m^i(t)\,\sigma_m(x)$$

- $\{\sigma_m\}_m$ a basis of $\mathbb{P}^k(\omega_i)$

Local variational formulation on ω_i

- $\displaystyle\int_{\omega_i} \left(\frac{\partial u}{\partial t} + \frac{\partial F(u)}{\partial x} \right) \psi \,\mathrm{d}x = 0$ with $\psi(x)$ a test function

Integration by parts

- $$\int_{\omega_i} \frac{\partial u}{\partial t}\psi \,\mathrm{d}x - \int_{\omega_i} F(u)\frac{\partial \psi}{\partial x}\,\mathrm{d}x + \Big[F(u)\,\psi\Big]_{x_{i-\frac{1}{2}}}^{x_{i+\frac{1}{2}}} = 0$$

Approximated solution

- Substitute u by u_h^i, and restrict ψ to the polynomial space $\mathbb{P}^k(\omega_i)$
- $$\int_{\omega_i} \frac{\partial \boldsymbol{u_h^i}}{\partial \boldsymbol{t}}\,\boldsymbol{\psi}\,\mathbf{d}\boldsymbol{x} = \int_{\omega_i} \boldsymbol{F}(\boldsymbol{u_h^i})\frac{\partial \boldsymbol{\psi}}{\partial \boldsymbol{x}}\,\mathbf{d}\boldsymbol{x} - \Big[\boldsymbol{\mathcal{F}}\,\boldsymbol{\psi}\Big]_{\boldsymbol{x_{i-\frac{1}{2}}}}^{\boldsymbol{x_{i+\frac{1}{2}}}}, \qquad \forall\, \boldsymbol{\psi} \in \mathbb{P}^{\boldsymbol{k}}(\boldsymbol{\omega_i})$$
- $$\sum_{m=1}^{k+1} \frac{\partial u_m^i}{\partial t} \int_{\omega_i} \sigma_m\,\sigma_p\,\mathrm{d}x = \int_{\omega_i} F(u_h^i)\frac{\partial \sigma_p}{\partial x}\,\mathrm{d}x - \Big[\mathcal{F}\,\sigma_p\Big]_{x_{i-\frac{1}{2}}}^{x_{i+\frac{1}{2}}}, \qquad \forall\, p \in [\![1, k+1]\!]$$

Numerical flux

- $$\mathcal{F}_{i+\frac{1}{2}} = \mathcal{F}\left(u_h^i(x_{i+\frac{1}{2}}, t), u_h^{i+1}(x_{i+\frac{1}{2}}, t)\right)$$
- $$\mathcal{F}(u, v) = \frac{F(u) + F(v)}{2} - \frac{\gamma(u, v)}{2}\,(v - u)$$
- $\gamma(u, v) = \max(|F'(u)|, |F'(v)|)$ Local Lax-Friedrichs

Subcell resolution of DG scheme

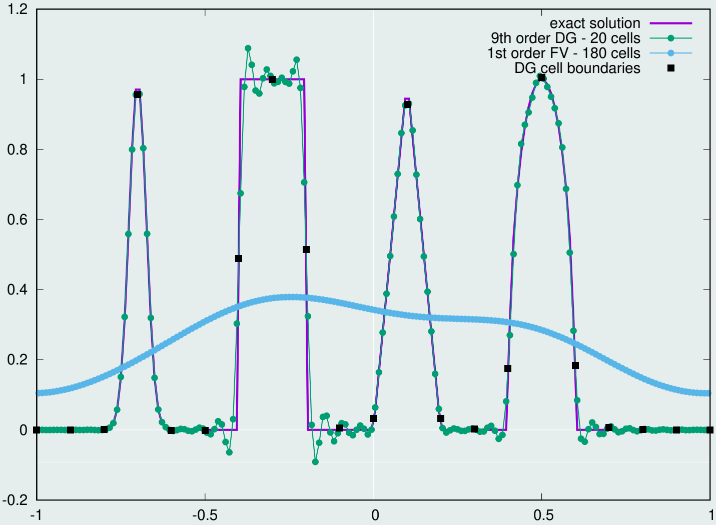

Figure : Linear advection of composite signal after 4 periods

Subcell resolution of DG scheme

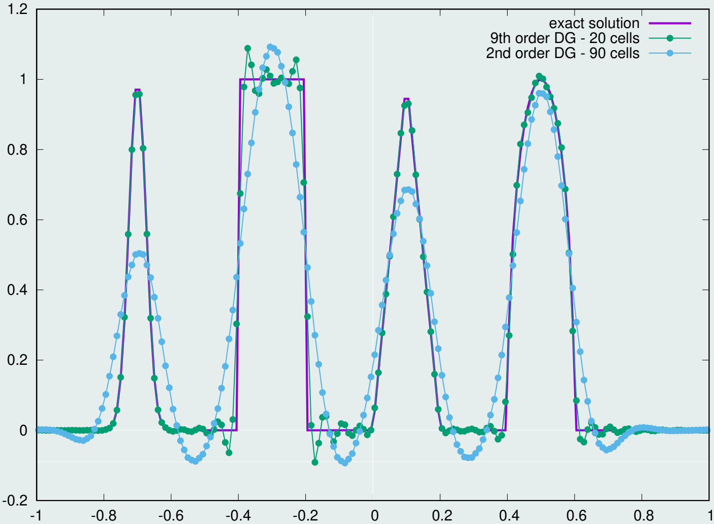

Figure : Linear advection of composite signal after 4 periods

Gibbs phenomenon

- High-order schemes leads to spurious oscillations near discontinuities
- Leads potentially to nonlinear instability, non-admissible solution, crash
- Vast literature of how prevent this phenomenon to happen:

$\Longrightarrow$ *a priori* and ***a posteriori*** limitations

A priori limitation

- Artificial viscosity
- Flux limitation
- Slope/moment limiter
- Hierarchical limiter
- ENO/WENO limiter

A posteriori limitation

- MOOD ("Multi-dimensional Optimal Order Detection")
- Subcell finite volume limitation
- **Subcell limitation through flux reconstruction**

Admissible numerical solution

- Maximum principle / positivity preserving
- Prevent the code from crashing (for instance avoiding NaN)
- **Ensure the conservation of the scheme**

Spurious oscillations

- Discrete maximum principle
- Relaxing condition for smooth extrema

Accuracy

- Retain as much as possible the subcell resolution of the DG scheme
- Minimize the number of subcell solutions to recompute

Modify locally, at the subcell level, the numerical solution without impacting the solution elsewhere in the cell

DG as a subcell finite volume

- Rewrite DG scheme as a specific finite volume scheme on subcells
- Exhibit the corresponding subcell numerical fluxes: **reconstructed flux**

Local variational formulation

- $\displaystyle\int_{\omega_i} \frac{\partial u_h^i}{\partial t}\,\psi\,\mathrm{d}x = \int_{\omega_i} F(u_h^i)\frac{\partial \psi}{\partial x}\,\mathrm{d}x - \Big[\mathcal{F}\,\psi\Big]_{x_{i-\frac{1}{2}}}^{x_{i+\frac{1}{2}}}, \qquad \forall\,\psi \in \mathbb{P}^k(\omega_i)$
- Substitute $F(u_h^i)$ with $F_h^i \in \mathbb{P}^{k+1}(\omega_i)$ (collocated or L_2 projection)
- $\displaystyle\int_{\omega_i} \frac{\partial u_h^i}{\partial t}\,\psi\,\mathrm{d}x = -\int_{\omega_i} \frac{\partial F_h^i}{\partial x}\,\psi\,\mathrm{d}x + \Big[(F_h^i - \mathcal{F})\,\psi\Big]_{x_{i-\frac{1}{2}}}^{x_{i+\frac{1}{2}}}, \qquad \forall\,\psi \in \mathbb{P}^k(\omega_i)$

Subcell decomposition through $k+2$ flux points

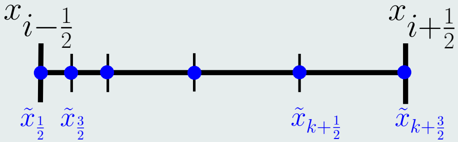

Subdivision and definition

- ω_i is subdivided in $k+1$ subcells $S_m^i = [\widetilde{x}_{m-\frac{1}{2}}, \widetilde{x}_{m+\frac{1}{2}}]$
- Let us define $\overline{\psi}_m = \dfrac{1}{|S_m^i|} \displaystyle\int_{S_m^i} \psi \, \mathrm{d}x$ the subcell mean value

Subresolution basis functions

- Let us introduce the $k+1$ basis functions $\{\phi_m\}_m$ such that $\forall\, \psi \in \mathbb{P}^k(\omega_i)$

$$\int_{\omega_i} \phi_m \, \psi \, \mathrm{d}x = \int_{S_m^i} \psi \, \mathrm{d}x, \qquad \forall\, m = 1, \dots, k+1,$$

- $\displaystyle\sum_{m=1}^{k+1} \phi_m(x) = 1$

These particular functions can be seen as the L_2 projection of the indicator functions $\mathbb{1}_m(x)$ onto $\mathbb{P}^k(\omega_i)$

Subcell finite volume scheme

- $\displaystyle \int_{\omega_i} \frac{\partial u_h^i}{\partial t} \phi_m \, \mathrm{d}x = -\int_{\omega_i} \frac{\partial F_h^i}{\partial x} \phi_m \, \mathrm{d}x + \Big[(F_h^i - \mathcal{F}) \, \phi_m \Big]_{x_{i-\frac{1}{2}}}^{x_{i+\frac{1}{2}}}$
- $\displaystyle |S_m^i| \frac{\partial \overline{u}_m^i}{\partial t} = -\int_{S_m^i} \frac{\partial F_h^i}{\partial x} \, \mathrm{d}x + \Big[(F_h^i - \mathcal{F}) \, \phi_m \Big]_{x_{i-\frac{1}{2}}}^{x_{i+\frac{1}{2}}}$
- $\displaystyle \frac{\partial \overline{u}_m^i}{\partial t} = -\frac{1}{|S_m^i|} \left(\Big[F_h^i \Big]_{\widetilde{x}_{m-\frac{1}{2}}}^{\widetilde{x}_{m+\frac{1}{2}}} - \Big[\phi_m \left(F_h^i - \mathcal{F} \right) \Big]_{x_{i-\frac{1}{2}}}^{x_{i+\frac{1}{2}}} \right)$
- $\displaystyle \frac{\partial \overline{u}_m^i}{\partial t} = -\frac{1}{|S_m^i|} \left(\widehat{F}^i_{m+\frac{1}{2}} - \widehat{F}^i_{m-\frac{1}{2}} \right)$ Subcell finite volume

Linear system

- $\displaystyle \widehat{F}^i_{m+\frac{1}{2}} - \widehat{F}^i_{m-\frac{1}{2}} = \Big[F_h^i \Big]_{\widetilde{x}_{m-\frac{1}{2}}}^{\widetilde{x}_{m+\frac{1}{2}}} - \Big[\phi_m \left(F_h^i - \mathcal{F} \right) \Big]_{x_{i-\frac{1}{2}}}^{x_{i+\frac{1}{2}}}, \qquad \forall\, m \in [\![1, k+1]\!]$
- $\widehat{F}^i_{\frac{1}{2}} = \mathcal{F}_{i-\frac{1}{2}}$ and $\widehat{F}^i_{k+\frac{3}{2}} = \mathcal{F}_{i+\frac{1}{2}}$

Reconstructed flux

- $\widehat{F}^i_{m+\frac{1}{2}} = F^i_h(\widetilde{x}_{m+\frac{1}{2}}) - C^{i-\frac{1}{2}}_{m+\frac{1}{2}} \left(F^i_h(x_{i-\frac{1}{2}}) - \mathcal{F}_{i-\frac{1}{2}} \right) - C^{i+\frac{1}{2}}_{m+\frac{1}{2}} \left(F^i_h(x_{i+\frac{1}{2}}) - \mathcal{F}_{i+\frac{1}{2}} \right)$
- $C^{i-\frac{1}{2}}_{m+\frac{1}{2}} = \sum_{p=m+1}^{k+1} \phi_p(x_{i-\frac{1}{2}})$ and $C^{i+\frac{1}{2}}_{m+\frac{1}{2}} = \sum_{p=1}^{m} \phi_p(x_{i+\frac{1}{2}})$

Correction terms for symmetric distribution of $\{\widetilde{x}_{m+\frac{1}{2}}\}_m$

- Let $\boldsymbol{B} \in \mathbb{R}^{k+1}$ be defined as $B_j = (-1)^{j+1} \binom{k+j}{j} \binom{k+1}{j}$
- $\widetilde{\xi}_{m+\frac{1}{2}} = \frac{\widetilde{x}_{m+\frac{1}{2}} - x_{i-\frac{1}{2}}}{x_{i+\frac{1}{2}} - x_{i-\frac{1}{2}}}, \quad \forall\, m = 0, \dots, k+1$
- $C^{i-\frac{1}{2}}_{m+\frac{1}{2}} = 1 - \left(\widetilde{\xi}_{m+\frac{1}{2}}, \dots, (\widetilde{\xi}_{m+\frac{1}{2}})^{k+1} \right)^{t} . \boldsymbol{B}$ and $C^{i+\frac{1}{2}}_{m+\frac{1}{2}} = C^{i-\frac{1}{2}}_{k+\frac{3}{2}-m}$

Subcell finite volume equivalent to DG

- $$\int_{\omega_i} \frac{\partial u_h^i}{\partial t}\,\psi\,\mathrm{d}x = \int_{\omega_i} F(u_h^i)\,\frac{\partial \psi}{\partial x}\,\mathrm{d}x - \Big[\mathcal{F}\,\psi\Big]_{x_{i-\frac{1}{2}}}^{x_{i+\frac{1}{2}}}, \qquad \forall\,\psi \in \mathbb{P}^k(\omega_i)$$
- $$\frac{\partial\,\overline{u}_m^i}{\partial t} = -\frac{1}{|S_m^i|}\left(\widehat{F}_{m+\frac{1}{2}}^i - \widehat{F}_{m-\frac{1}{2}}^i\right), \qquad \forall\, m = 1,\dots,k+1$$
- $$\widehat{F}_{m+\frac{1}{2}}^i = F_h^i(\widetilde{x}_{m+\frac{1}{2}}) - C_{m+\frac{1}{2}}^{i-\frac{1}{2}}\left(F_h^i(x_{i-\frac{1}{2}}) - \mathcal{F}_{i-\frac{1}{2}}\right) - C_{m+\frac{1}{2}}^{i+\frac{1}{2}}\left(F_h^i(x_{i+\frac{1}{2}}) - \mathcal{F}_{i+\frac{1}{2}}\right)$$

Reconstructed flux taking into account flux jumps

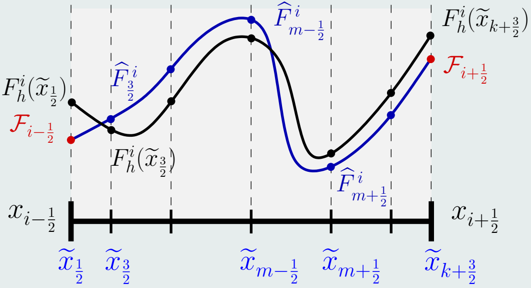

Flux reconstruction / CPR

- The correction functions defined as

$$g_{LB}(x) = \sum_{m=0}^{k+1} C^{(m)}_{i-\frac{1}{2}}\, L_m(x) \quad \text{and} \quad g_{RB}(x) = \sum_{m=0}^{k+1} C^{(m)}_{i+\frac{1}{2}}\, L_m(x)$$

are nothing but the right and left Radau $\mathbb{P}^k$ polynomials

H. T. Huynh, *A Flux Reconstruction Approach to High-Order Schemes Including Discontinuous Galerkin Methods.* 18th AIAA Computational Fluid Dynamics Conference Miami, 2007.

Z.J. Wang and H. Gao, *A unifying lifting collocation penalty formulation including the discontinuous Galerkin, spectral volume/difference methods for conservation laws on mixed grids.* JCP, 2009.

Subcell finite volume

- Reconstructed flux is used as a numerical flux for subcell FV schemes
- This demonstration is not restricted to the flux collocation case
- The correction terms are very simple and explicitly defined

RKDG scheme

- SSP Runge-Kutta: convex combinations of first-order forward Euler
- For sake of clarity, we focus on forward Euler time stepping

Projection on subcells of RKDG solution

- $u_h^{i,n}(x) = \displaystyle\sum_{m=1}^{k+1} u_m^{i,n}\,\sigma_m(x)$ is uniquely defined by its $k+1$ submean values
- Introducing the matrix Π defined as $\pi_{mp} = \dfrac{1}{|S_m^i|}\displaystyle\int_{S_m^i} \sigma_p \,\mathrm{d}x,$ then

$$\Pi \begin{pmatrix} u_1^{i,n} \\ \vdots \\ u_{k+1}^{i,n} \end{pmatrix} = \begin{pmatrix} \overline{u}_1^{i,n} \\ \vdots \\ \overline{u}_{k+1}^{i,n} \end{pmatrix}$$

Projection

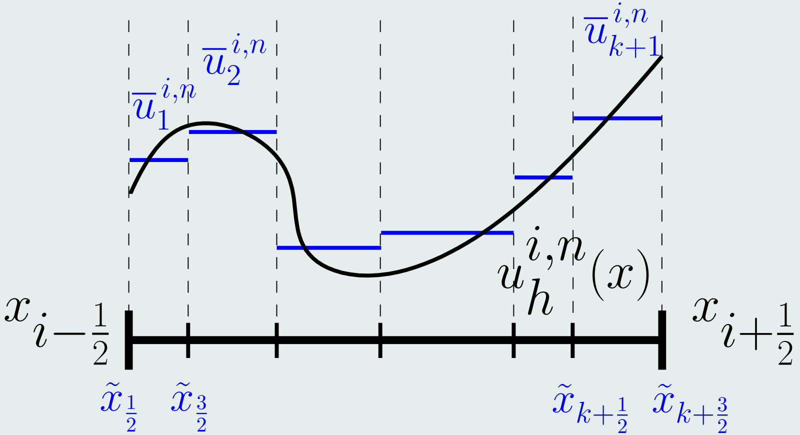

Figure : Polynomial solution and its associated submean values

Set up

- We assume that, for each cell, the $\{\overline{u}_m^{i,n}\}_m$ are admissible
- Compute a candidate solution u_h^{n+1} from u_h^n through uncorrected DG
- For each subcell, check if the submean values $\{\overline{u}_m^{i,n+1}\}_m$ are ok

Physical admissibility detection (PAD)

- Check if $\overline{u}_m^{i,n+1}$ lies in an convex physical admissible set (maximum principle for SCL, positivity of the pressure and density for Euler, . . .)
- Check if there is any *NaN* values

Numerical admissibility detection (NAD)

- Discrete maximum principle DMP on submean values:

$$\min_p(\overline{u}_p^{i-1,n}, \overline{u}_p^{i,n}, \overline{u}_p^{i+1,n}) \leq \overline{u}_m^{i,n+1} \leq \max_p(\overline{u}_p^{i-1,n}, \overline{u}_p^{i,n}, \overline{u}_p^{i+1,n})$$

- This criterion needs to be relaxed to preserve smooth extrema

Corrected reconstructed flux

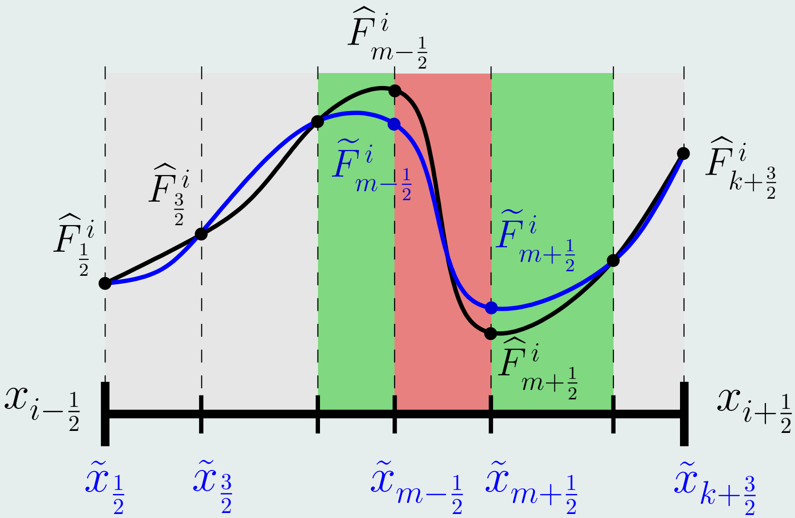

Figure : Correction of the reconstructed flux

Flowchart

1. Compute the uncorrected DG candidate solution $u_h^{i,n+1}$
2. Project $u_h^{i,n+1}$ to get the submean values $\overline{u}_m^{i,n+1}$
3. Check $\overline{u}_m^{i,n+1}$ through the troubled zone detection plus relaxation
4. If $\overline{u}_m^{i,n+1}$ is admissible go further in time, otherwise modify the corresponding reconstructed flux values

$$\widetilde{F}^i_{m-1} = \mathcal{F}(\overline{u}^{i,n}_{m-1}, \overline{u}^{i,n}_m) \quad \text{and} \quad \widetilde{F}^i_m = \mathcal{F}(\overline{u}^{i,n}_m, \overline{u}^{i,n}_{m+1})$$

5. Through the corrected reconstructed flux, recompute the submean values for tagged subcells and their first neighbors
6. Return to 3

Conclusion

- The limitation only affects the DG solution at the subcell scale
- The corrected scheme is conservative at the subcell level
- In practice, few submean values need to be recomputed

Initial solution on $x \in [0,1]$

- $u_0(x) = \sin(2\pi x)$
- Periodic boundary conditions

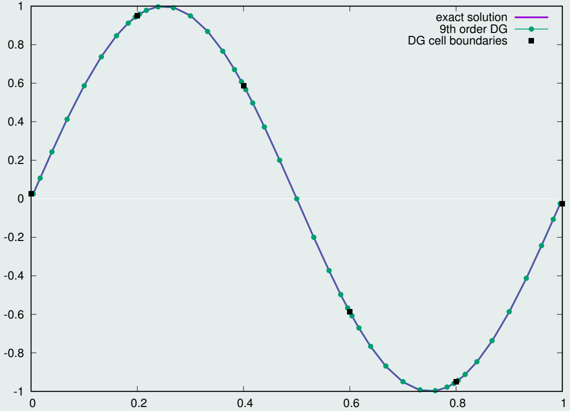

Figure : Linear advection with a 9th DG scheme and 5 cells after 1 period

Convergence rates

	L_1		L_2	
h	$E_{L_1}^h$	$q_{L_1}^h$	$E_{L_2}^h$	$q_{L_2}^h$
$\frac{1}{20}$	8.07E-11	9.00	8.97E-11	9.00
$\frac{1}{40}$	1.58E-13	9.00	1.75E-13	9.00
$\frac{1}{80}$	3.08E-16	-	3.42E-16	-

Table: Convergence rates for the linear advection case for a 9th order DG scheme

Linear advection of a square signal after 1 period

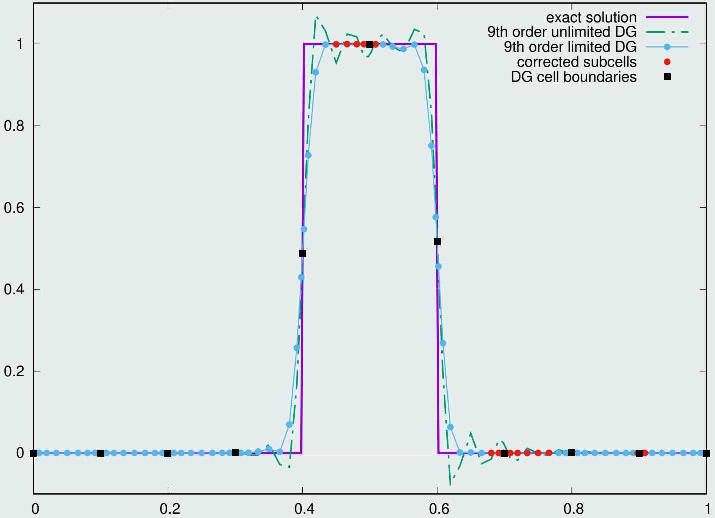

Figure : 9th order corrected and uncorrected DG solutions

Linear advection of a square signal after 10 periods

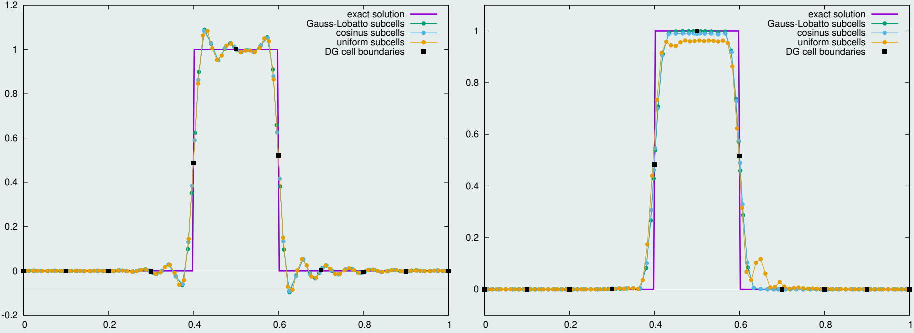

(a) Without correction (b) With correction

Figure : Comparison between different cell subdivision

Linear advection of a square signal

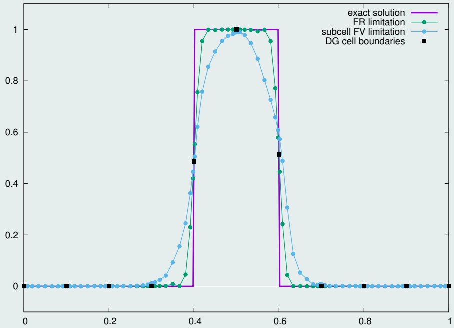

(a) After 1 period

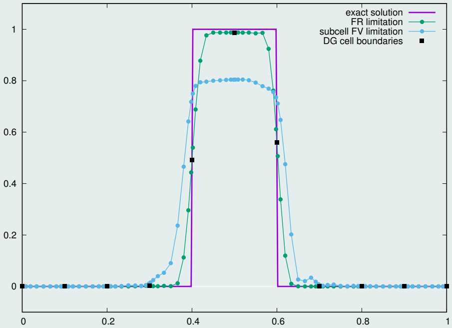

(b) After 50 periods

Figure : Comparison between subcell FV limitation and the present correction

Linear advection of a square signal

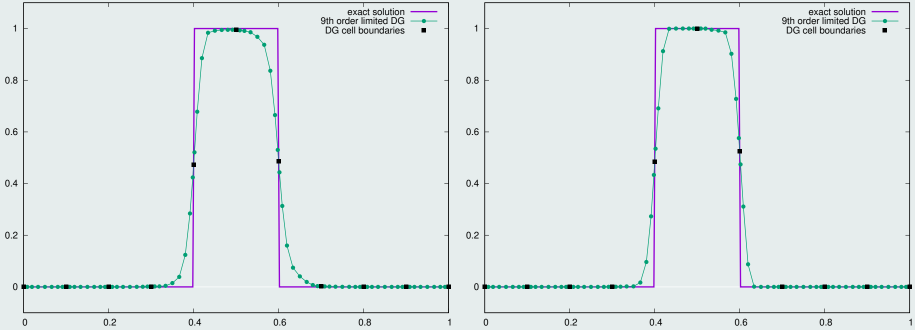

(a) 1st-order correction

(b) 2nd-order correction

Figure : Comparison between 1st and 2nd order correction for the SubNAD detection criterion

Linear advection of a composite signal after 4 periods

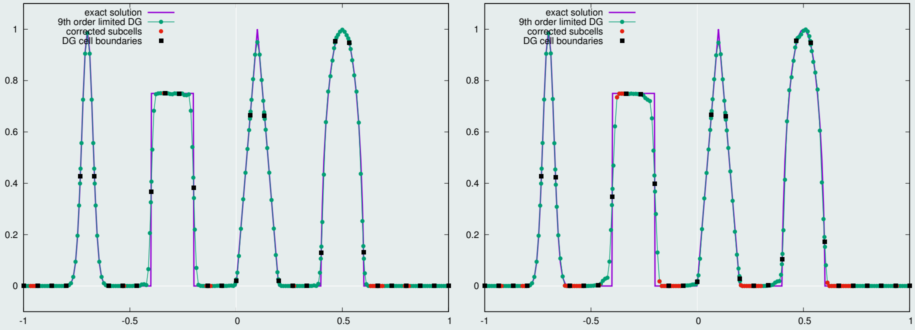

(a) NAD and 1st-order correction

(b) SubNAD and 2nd-order correction

Figure : 9th order corrected DG on 30 cells

Linear advection of a composite signal after 4 periods

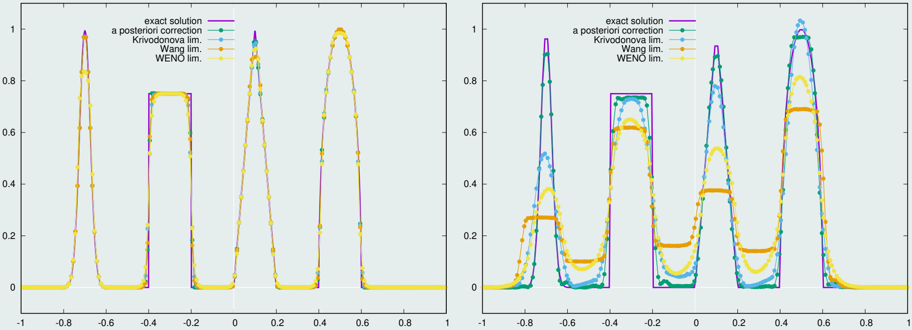

(a) 200 cells: cell mean values (b) 50 cells: subcell mean values

Figure : 4th order DG solutions provided different limitations

Linear advection of a composite signal after 4 periods

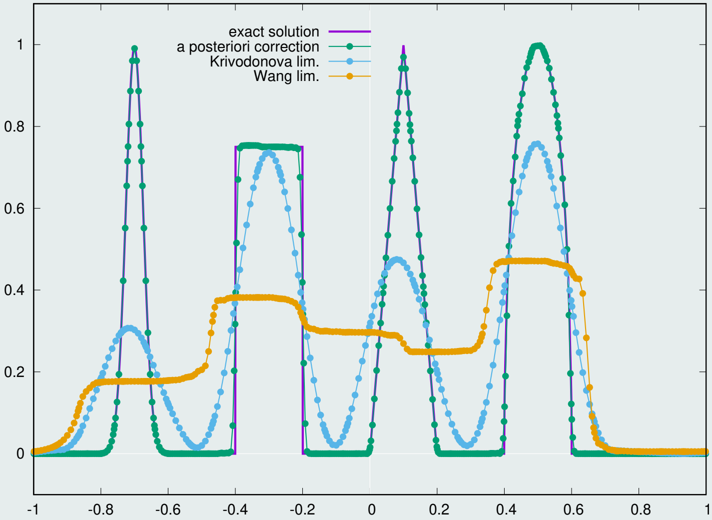

Figure : 9th order DG solutions provided different limitations on 30 cells

Burgers equation: $u_0(x) = \sin(2\pi\, x)$

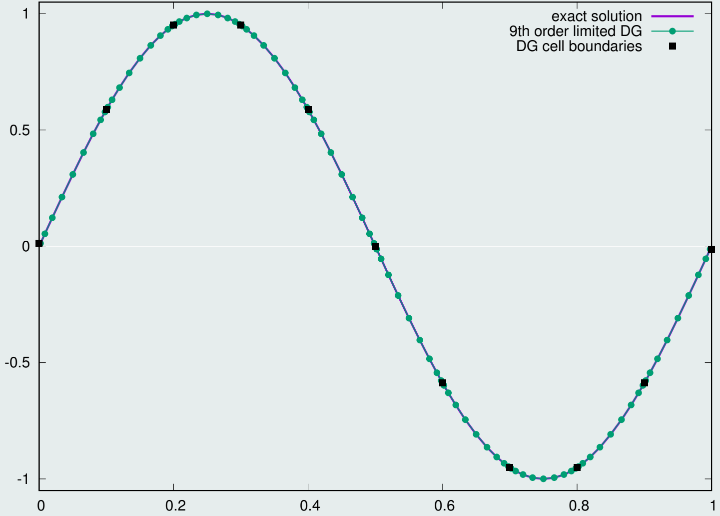

Figure : 9th order corrected DG on 10 cells for $t_f = 0.7$

Burgers equation: expansion and shock waves collision

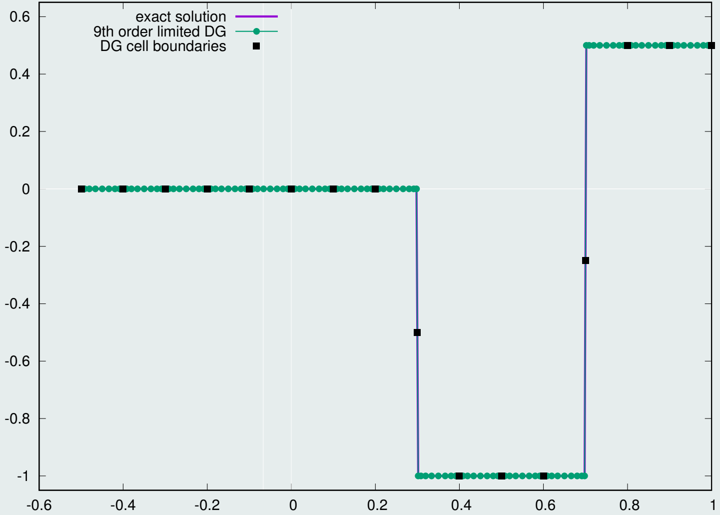

Figure : 9th order corrected DG on 15 cells for $t_f = 1.2$

Burgers equation: expansion and shock waves collision

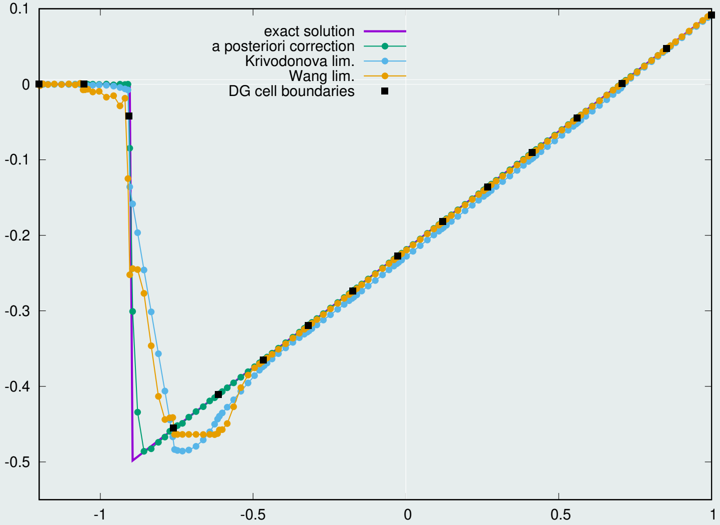

Figure : 9th order corrected DG on 15 cells provided different limitations

Buckley non-convex flux problem at time $t = 0.4$

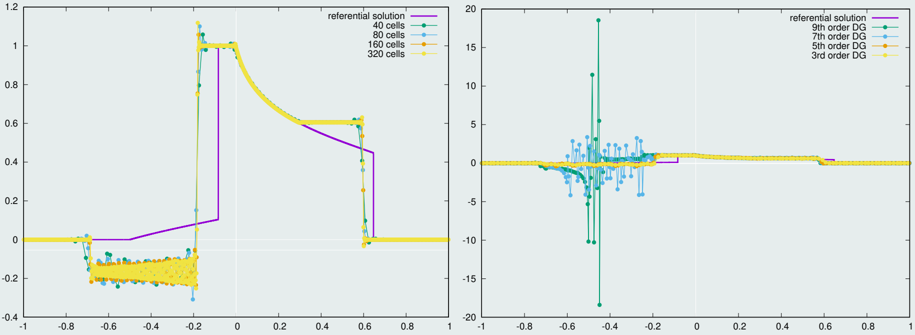

(a) Non-entropic behavior (b) Aliasing phenomenon

Figure : Uncorrected DG solution for the Buckley non-convex flux case

Buckley non-convex flux problem at time $t = 0.4$

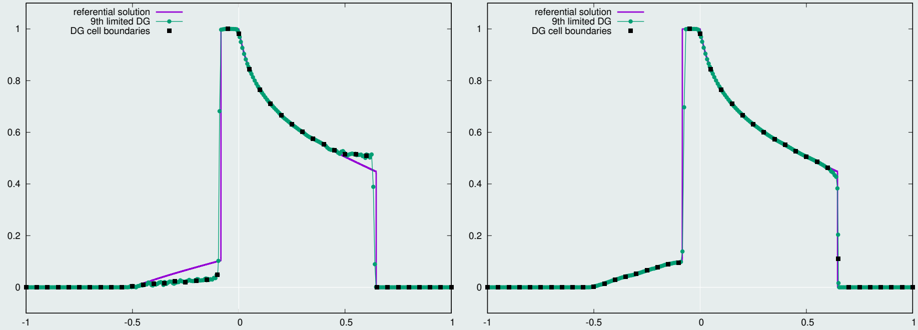

(a) NAD criterion (b) SubNAD criterion

Figure : 9th order DG solutions on 40 cells

Buckley non-convex flux problem at time $t = 0.4$

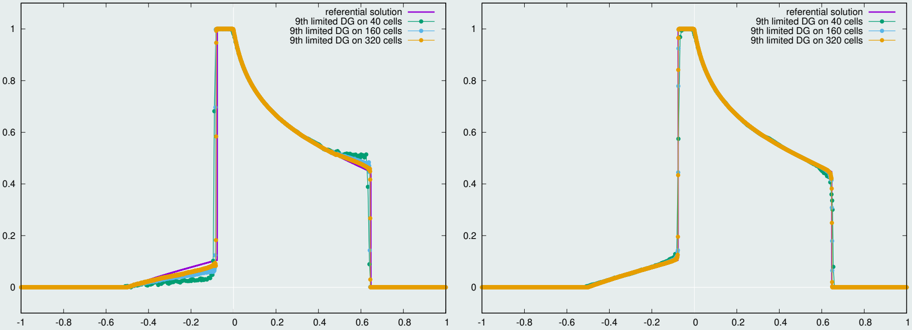

(a) NAD criterion

(b) SubNAD criterion

Figure : Convergence analysis of 9th order DG scheme

Buckley non-convex flux problem at time $t = 0.4$

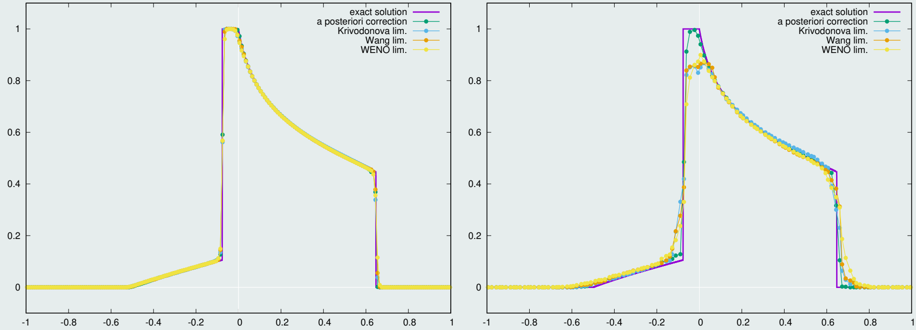

(a) 200 cells: cell mean values

(b) 30 cells: subcell mean values

Figure : 4th order DG solutions provided different limitations

Buckley non-convex flux problem at time $t = 0.4$

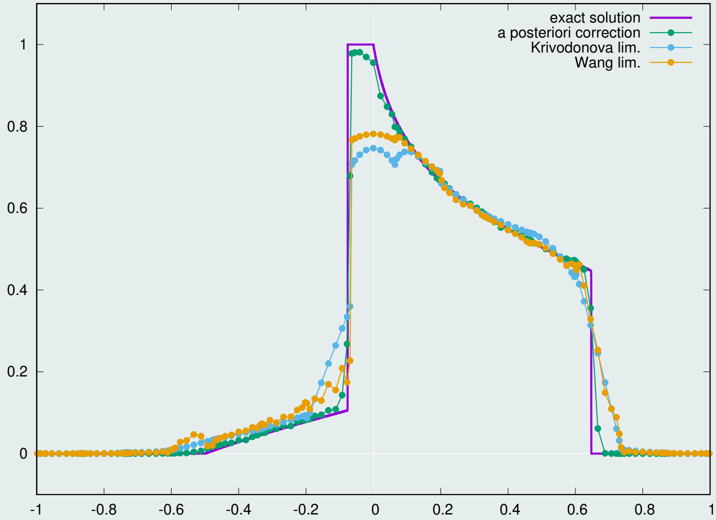

Figure : 9th order DG solutions provided different limitations on 15 cells

Initial solution on $x \in [0,1]$ for $\gamma = 3$

- $\rho_0(x) = 1 + 0.9999999\sin(\pi x), \quad u_0(x) = 0, \quad p_0(x) = (\rho_0(x))^\gamma$

$$\Longrightarrow \rho_0(-\tfrac{1}{2}) = 1.E-7 \quad \text{and} \quad p_0(-\tfrac{1}{2}) = 1.E-21$$

- Periodic boundary conditions

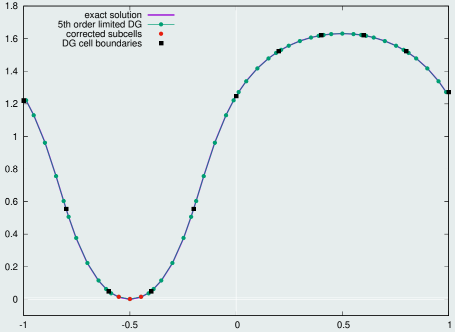

(a) Density (b) Internal energy

Figure : 5th order corrected DG solution on 10 cells at $t = 0.1$

Convergence rates

h	L_1: $E^h_{L_1}$	L_1: $q^h_{L_1}$	L_2: $E^h_{L_2}$	L_2: $q^h_{L_2}$	Average % of corrected subcells
$\frac{1}{20}$	1.48E-5	4.35	2.02E-5	4.18	6.87 %
$\frac{1}{40}$	9.09E-7	4.88	1.38E-6	4.87	3.31 %
$\frac{1}{80}$	3.09E-8	4.95	4.73E-8	4.86	2.50 %
$\frac{1}{160}$	1.00E-9	-	1.63E-9	-	1.12 %

Table: Convergence rates on the pressure for the Euler equation for a 5th order DG

Sod shock tube problem

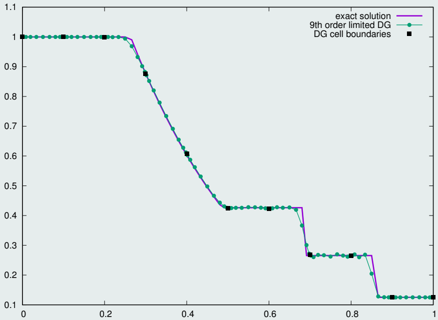

(a) NAD + 1st order correction

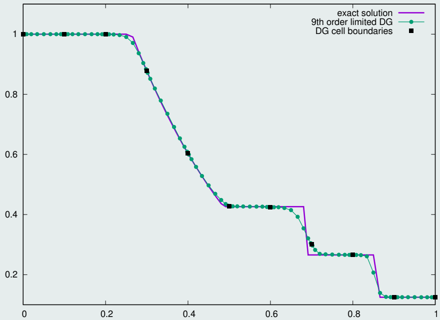

(b) SubNAD + 2nd order correction

Figure : 9th order corrected DG on 10 cells

Sod shock tube problem

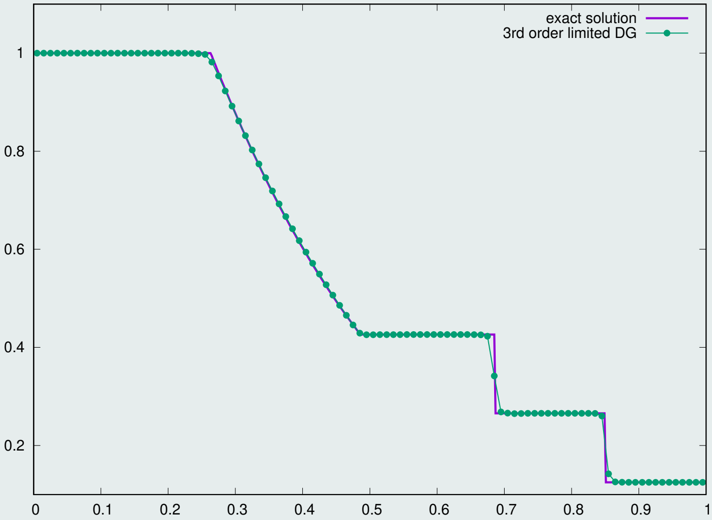

Figure : 3rd order DG solutions on 100 cells: cell mean values

Shock acoustic-wave interaction problem

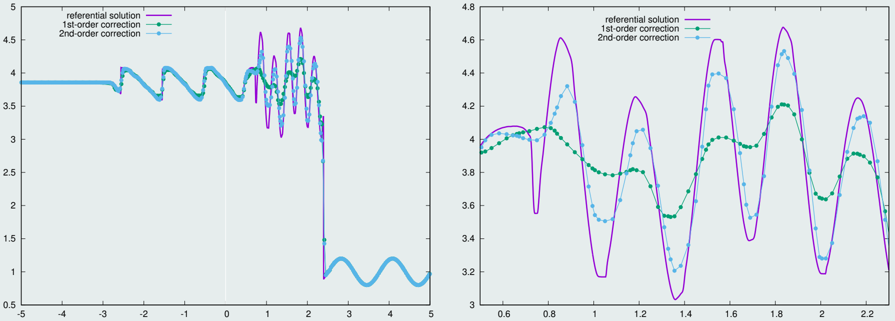

(a) Global view (b) Zoom on $[0.5, 2.3]$

Figure : 7th order corrected DG on 50 cells: comparison between 1st and 2nd order corrections

Shock acoustic-wave interaction problem

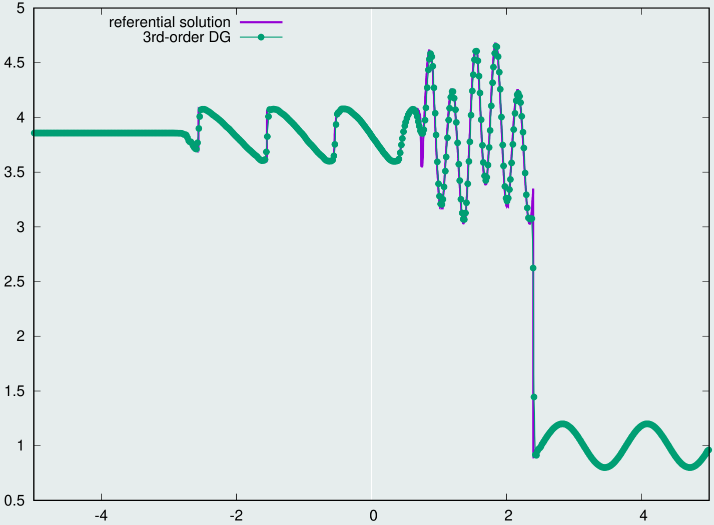

Figure : 3rd order corrected DG solutions on 200 cells: cell mean values

Blast waves interaction problem

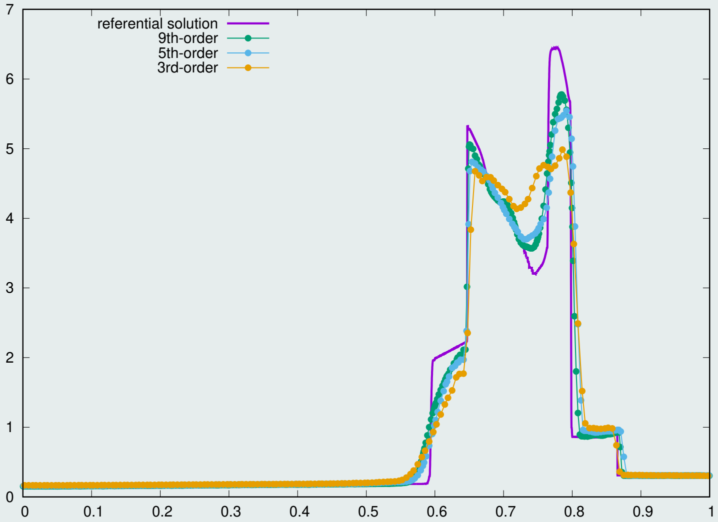

Figure : Corrected DG solution on 60 cells, from 3rd to 9th order

2D grid and subgrid

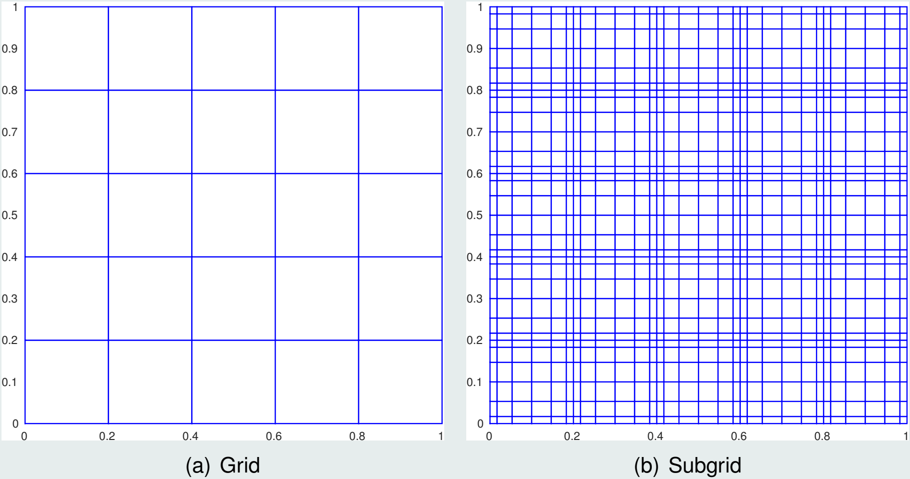

Figure : 5x5 Cartesian grid and corresponding subgrid for a 6th order DG scheme

Initial solution on $(x, y) \in [0, 1]^2$

- $u_0(x, y) = \sin(2\pi(x + y))$
- Periodic boundary conditions

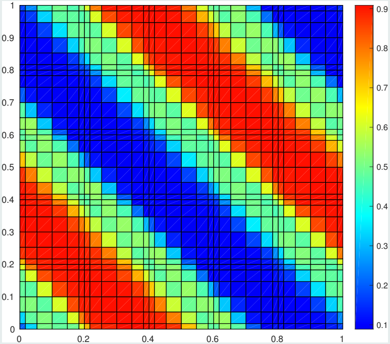

(a) Solution map

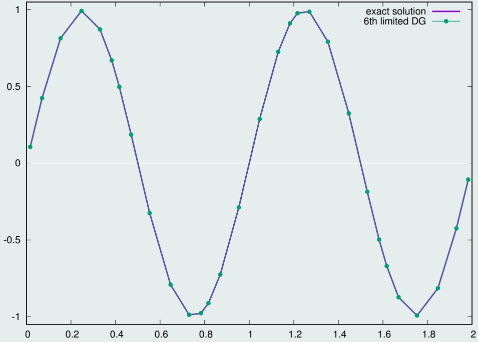

(b) Solution profile

Figure : Linear advection with a 6th DG scheme and 5x5 grid after 1 period

Convergence rates

	L_1		L_2	
h	$E_{L_1}^h$	$q_{L_1}^h$	$E_{L_2}^h$	$q_{L_2}^h$
$\frac{1}{5}$	2.10E-6	6.23	2.86E-6	6.24
$\frac{1}{10}$	2.79E-8	6.00	3.77E-8	6.00
$\frac{1}{20}$	3.36E-10	-	5.91E-10	-

Table: Convergence rates for the linear advection case for a 6th order DG scheme

Rotation of a composite signal after 1 period

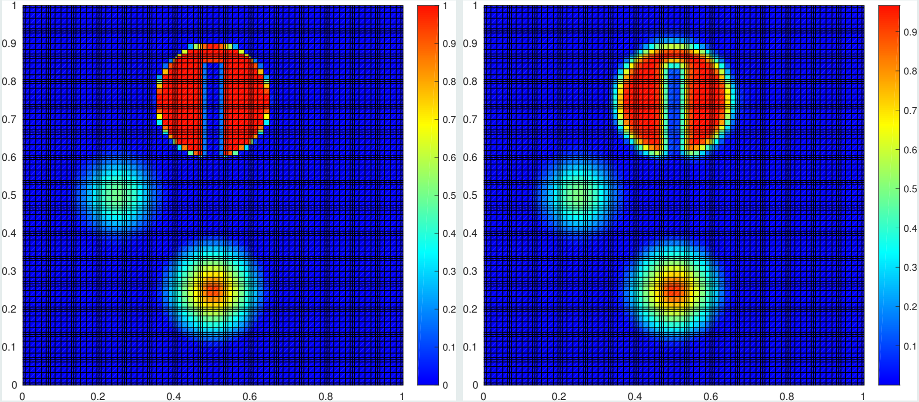

(a) Initial solution

(b) Final solution

Figure : 6th order corrected DG on a 15x15 Cartesian mesh

Rotation of a composite signal after 1 period

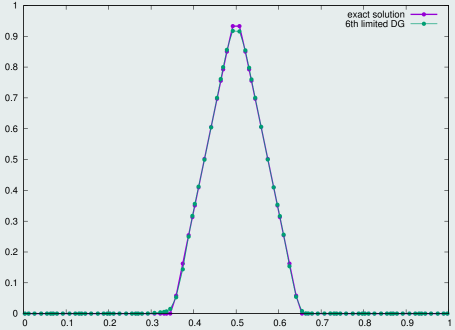

(a) Solution profile for $y = 0.25$ (b) Solution profile for $y = 0.75$

Figure : 6th order corrected DG on a 15x15 Cartesian mesh

Rotation of a composite signal after 1 period: $x = 0.25$

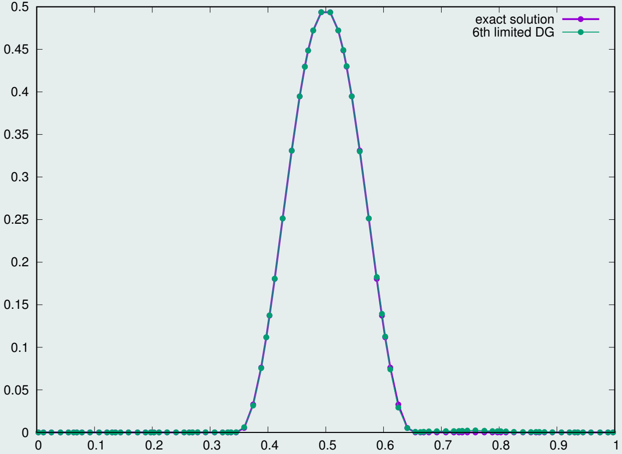

Figure : 6th order corrected DG on a 15x15 Cartesian mesh

Burgers equation with $u_0(x, y) = \sin(2\pi (x + y))$

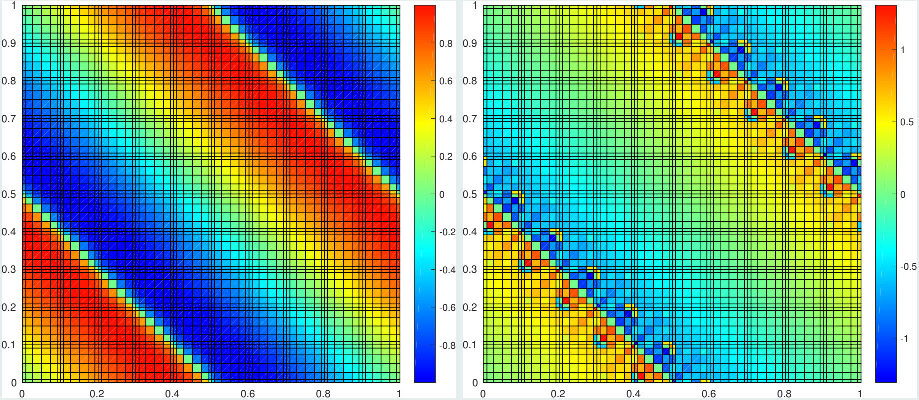

(a) Solution at $t = 0.007$ (b) Solution at $t = 0.25$

Figure : 6th order uncorrected DG on a 10x10 Cartesian mesh

Burgers equation with $u_0(x, y) = \sin(2\pi\,(x + y))$

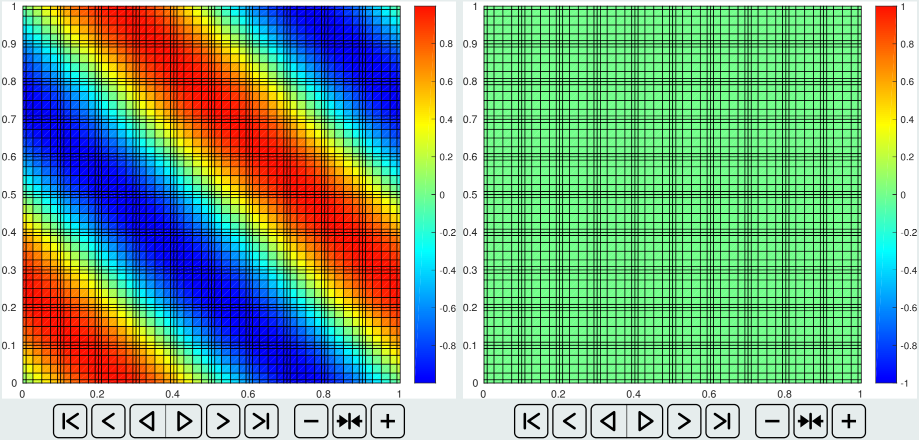

(a) Solution map (b) Detected subcells

Figure : 6th order corrected DG on a 10x10 Cartesian mesh until $t = 0.5$

Burgers equation with $u_0(x, y) = \sin(2\pi\,(x + y))$ at $t = 0.5$

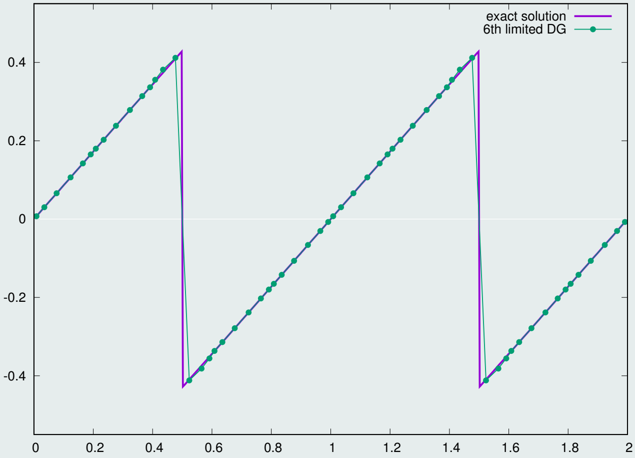

Figure : 6th order corrected DG solution profile on a 10x10 Cartesian mesh

Burgers equation with composite signal

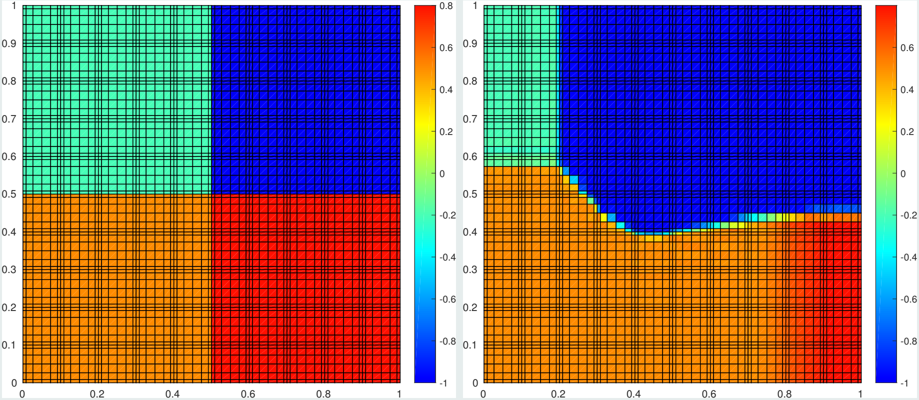

(a) Initial solution

(b) Solution at $t = 0.5$

Figure : 6th order corrected DG on a 10x10 Cartesian mesh

Kurganov, Petrova, Popov (KPP) non-convex flux problem

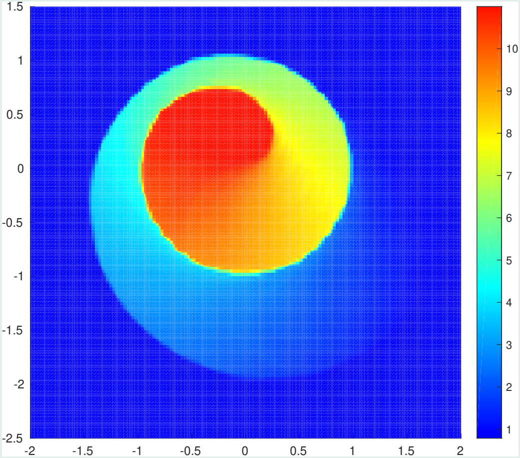

Figure : 6th order corrected DG solution on a 30x30 Cartesian mesh

Ongoing work

- Extension to unstructured grids
- Maximum principle preserving DG scheme through subcell FCT reconstructed flux
- DoF based *h-p* adaptive DG scheme through subcell finite volume formulation

Published paper

F. VILAR, *A Posteriori Correction of High-Order Discontinuous Galerkin Scheme through Subcell Finite Volume Formulation and Flux Reconstruction.* JCP, (15)245-279, 2018.

Relaxation of the DMP

- $v_L = \overline{\partial_x u}_i^{n+1} - \frac{\Delta x_i}{2}\,\overline{\partial_{xx} u}_i^{n+1}$
- $v_{\min \setminus \max} = \min \setminus \max\,(\overline{\partial_x u}_i^{n+1}, \overline{\partial_x u}_{i-1}^{n+1})$
- If $(v_L > \overline{\partial_x u}_i^{n+1})$ Then $\alpha_L = \min(1, \dfrac{v_{\max} - \overline{\partial_x u}_i^{n+1}}{v_R - \overline{\partial_x u}_i^{n+1}})$
- If $(v_L < \overline{\partial_x u}_i^{n+1})$ Then $\alpha_L = \min(1, \dfrac{v_{\min} - \overline{\partial_x u}_i^{n+1}}{v_R - \overline{\partial_x u}_i^{n+1}})$

- $v_R = \overline{\partial_x u}_i^{n+1} + \frac{\Delta x_i}{2}\,\overline{\partial_{xx} u}_i^{n+1}$
- $v_{\min \setminus \max} = \min \setminus \max\,(\overline{\partial_x u}_i^{n+1}, \overline{\partial_x u}_{i+1}^{n+1})$
- If $(v_R > \overline{\partial_x u}_i^{n+1})$ Then $\alpha_R = \min(1, \dfrac{v_{\max} - \overline{\partial_x u}_i^{n+1}}{v_R - \overline{\partial_x u}_i^{n+1}})$
- If $(v_R < \overline{\partial_x u}_i^{n+1})$ Then $\alpha_R = \min(1, \dfrac{v_{\min} - \overline{\partial_x u}_i^{n+1}}{v_R - \overline{\partial_x u}_i^{n+1}})$

Relaxation of the DMP

- $\alpha = \min(\alpha_L, \alpha_R)$
- If $(\alpha = 1)$ Then DMP is relaxed

Hierarchical limiter

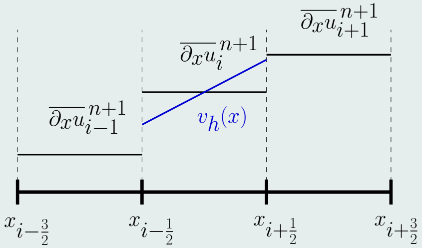

- $v_h(x) = \overline{\partial_x u}_i^{n+1} + (x - x_i)\,\overline{\partial_{xx} u}_i^{n+1}$

M. Yang and Z.J. Wang, *A parameter-free generalized moment limiter for high-order methods on unstructured grids.* AAMM., 2009.

D. Kuzmin, *A vertex-based hierarchical slope limiter for p-adaptive discontinuous Galerkin methods.* J. of Comp. and Appl. Math., 2010.

Linear advection of a square signal after 1 period

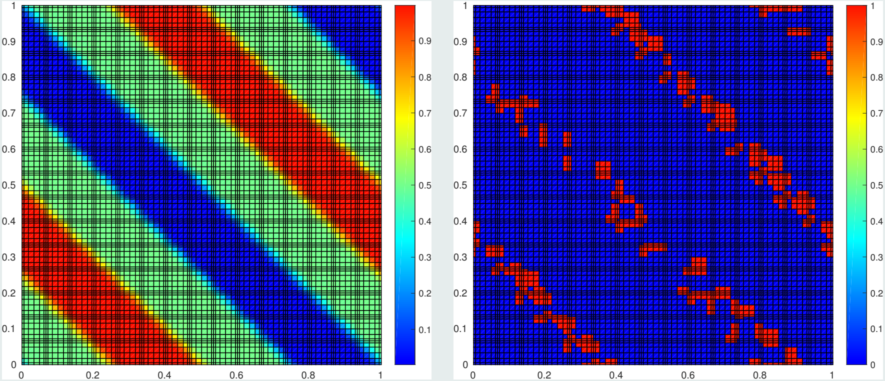

(a) Solution map (b) Solution profile

Figure : 6th order corrected DG on a 15x15 Cartesian mesh

Linear advection of a square signal after 1 period

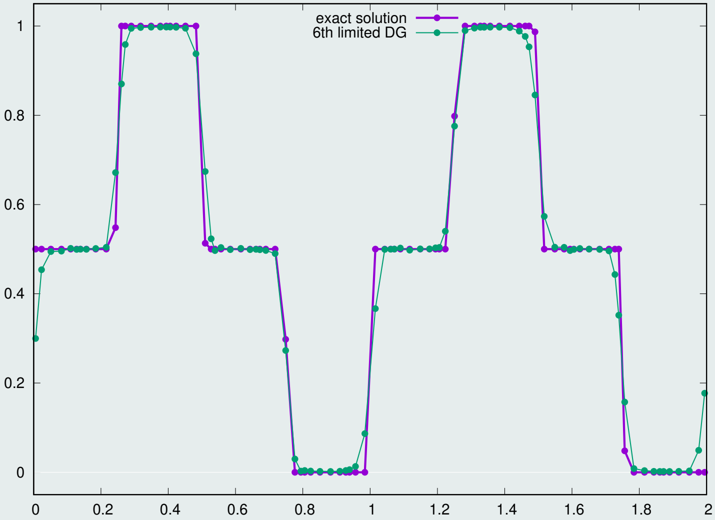

Figure : 6th order corrected DG on a 15x15 Cartesian mesh